Journal of Applied Sciences

ISSN 1812-5654

science alert

ANSInet
an open access publisher
http://ansinet.com

Journal of Applied Sciences 6 (7): 1426-1436, 2006
ISSN 1812-5654

Laminar Natural Convection in a Vertical Channel with a Sinusoidal Obstruction

[1]Belkacem Abdellah, [1]Rebhi Mebrouk, [1]Draoui Belkacem and [2]Chikh Salah
[1]Institut de Génie Mécanique, C.U.Béchar, Béchar., Algérie
[2]Faculté de Génie Mécanique et Génie des Procédés, USTHB, Alger, Algérie

Abstract: In this study, a numerical study of laminar natural convection flow of air in a vertical channel with only one sinusoidal obstruction is performed. The wall containing the obstruction is assumed to be heated while the other wall is assumed to be adiabatic (asymmetric heating). The governing elliptic equations are discretized in a two dimensional domain using the finite-volume method with non-staggered variable arrangement and the PISO algorithm for the velocity-pressure coupling is employed. Simulation was carried out for a range of amplitude of the sinusoidal obstruction a = 0.0-0.5, aspect ratio A = 5, channel Rayleigh number $Ra^* = 10^2$ to 2.10^5 for a fluid having Prandtl number equal to 0.71. Streamlines and isothermal lines represent the corresponding flow and thermal fields. Local and global Nusselt number distributions express the rate of heat transfer.

Key words: Natural convection, asymmetric heating, sinusoidal obstruction, control volume method

INTRODUCTION

The two-dimensional laminar natural convection flow of air in a vertical channel made object of many theoretical and experimental work because of its implication in a number of natural phenomena and industrial processes as varied as the habitat, drying, the heat exchangers, electronics, etc. We distinguish the three following cases:

- Two-dimensional laminar natural convection in a vertical channel formed by two parallel plates (Elenbaas, 1942; Ostrach, 1952; Bodoia and Osterle, 1962; Engel and Mueller, 1967; Aung *et al*., 1972; Aung, 1972; Hugot, 1972; Aihara, 1973; Miyatake and Fujii, 1972; Akbari and Borges, 1979; Dalbert *et al*., 1981; Wirtz and Stutzman, 1982; Sparrow *et al*., 1984; Sparrow and Azevedo, 1985; Webb and Hill, 1989).
- Laminar natural convection flow in a two-dimensional vertical channel, but with an imposed particular condition, either in the configuration of the channel, or in the way of tackling the problem (Dyer and Fowler, 1966; Kettleborough, 1972; Dyer, 1975, 1978; Nakamura *et al*., 1982; Sparrow and Tao, 1982; Agonaffer and Watkins, 1985; Azevedo and Sparrow, 1986; Sparrow *et al*.,1988; Sparrow and Ruiz, 1988).
- Laminar and two-dimensional mixed convection flow in a vertical channel (Dalbert *et al*., 1980; Penot and Dalbert, 1983; Aung and Worku, 1986a, b; Habchi and Acharrya, 1986).

Most of these studies relate to the case where the walls are maintained at a constant temperature and are based on a parabolic formulation of the equations in which the axial diffusion is neglected. The conditions of uniform heat flux on the walls were initially studied by Engel and Mueller, 1967 followed by Aung *et al*. (1972), Dalbert *et al*. (1981), Writz and Stutzman (1982), Dyer (1975), Penot and Dalbert (1983).

Bar-Cohen and Resenhow (1984) worked out starting from the experimental and numerical results their predecessors, a whole of correlations characterizing the heat transfer in a channel whose walls are symmetrically or asymmetrically heated by a uniform heat flux or maintained at temperatures.

Naylor *et al*. (1991) were among the first to solve the complete Navier-Stokes equations and to show the influence with low numbers Rayleigh of one extension to the entry of channel.

It can be observed that the motion pressure at the entry of the channel was considered a long time as equal to that reigning outside. This assumption neglects the influence of the pressure at the entry due to the fluid acceleration. Aihara (1973) is one of the first which studied the influence of inlet conditions of pressure and the velocity profile within an isothermal vertical channel. Dalbert *et al*. (1981) confirms the influence of the inlet conditions of pressure within an vertical channel asymmetrically heated with uniform heat flux, while being based on the results of the limits cases (Aung, 1972).

Corresponding Author: Belkacem Abdellah, Institut de Génie Mécanique, C.U. Béchar, Algérie

Recently, Marcondes and Maliska (1999) numerically demonstrated in an asymmetrically heated channel, that using the inlet motion pressure $P_m = -0.5Q^2$ instead of $P_m = 0$, has no noticeable influence on the mean Nusselt number but substantially decreases the mass flow rate.

The natural convection in vertical channel with roughness elements has been less frequently reported in the literature, even though it is encountered in several technological applications. In such circumstances the natural convective flow may be significantly altered by roughness elements mounted on the channel surfaces.

Habchi and Acharya (1986) numerically investigated the laminar mixed convection of air in a vertical channel with a single rectangular rib. They demonstrated that for a symmetrically heated channel the mean Nusselt numbers are smaller then the corresponding smooth channel Nusselt numbers, i.e. for an unobstructed channel. Mehrotra and Acharya (1993) conducted an experimental study of natural convection heat transfer in smooth and ribbed UWT and UHF vertical channels. Said and Krane (1990) preformed a numerical and experimental investigation of natural convection in a vertical channel with a single semi-circular obstacle. They showed that the location of the rib along the wall affects the rate of heat transfer. A free convection flows in vertical channel with two rectangular obstructions on opposite walls was studied numerically by Viswatmula and Ruhul Amin (1995). They found that the average Nusselt numbers for obstructed channels are less than those of the smooth channel.

Desrayaud and Fichera (2002) numerically investigated the laminar natural convective flows in a vertical channel with two symmetrical isothermal or adiabatic ribs. They found that the mean Nusselt number at high Rayleigh number is very similar for isothermal and adiabatic ribs whatever their location.

Hadjadj and Kyal (1999) numerically investigated the effect of sinusoidal protuberances on heat transfer and fluid flow inside an annular space using a non-orthogonal coordinate transformation. They reported that the both local and average heat transfer increase with the increase of protuberances amplitude and Rayleigh number and decreasing Prandtl number.

Obviously, further numerical studies of the problem of the natural convection in obstructed channel with different geometries are necessary. Thus, the objective of this study is to numerically investigate the natural convection in an asymmetrically heated vertical channel with a sinusoidal obstruction and to study the effect of obstruction amplitude, location of the obstruction and aspect ratio of the channel on heat transfer and fluid flow.

MATHEMATICAL MODELING

In the proposed study, we consider a vertical two dimensional channel formed by two plates of height H separated by a distance d. Left plate of the channel is flat and adiabatic; the right plate is maintained at uniform temperature and obeys at the following law (Fig.1):

$$Y = F(X) = 1 \qquad \text{if} \quad L_0+L_1 \le X \le L_1$$

$$Y = F(X) = 1\text{-}a\sin \pi/L_0\ (X\text{-}L_1) \qquad \text{if} \quad L_1 \le X \le L_0+L_1 \tag{1}$$

The wavy obstruction is located at a distance L1 downstream of the channel inlet. The local distance X along the channel is measured from the leading edge of the left plate of the channel.

The flow is considered steady-state, laminar and incompressible with no internal heat generation and the Boussinesq approximation has been applied. Other valid assumptions are that the compression work, viscous dissipation and radiative transport are negligibly small.

The governing equations for the flow in a vertical channel are parabolic in nature. But the presence of recirculating flows in the vertical obstruction channel makes these governing equations elliptic. With these assumptions, the governing equations can be written in the following dimensionless form:

Conservation of mass:

$$\frac{\partial U}{\partial X} + \frac{\partial V}{\partial Y} = 0 \tag{2}$$

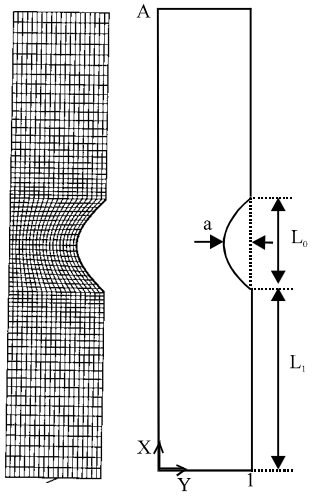

Fig. 1: Schematic diagram of the problem under consideration

Conservation of momentum:

$$\frac{\partial U}{\partial t}+U\frac{\partial U}{\partial X}+V\frac{\partial U}{\partial Y}=-\frac{\partial P_m}{\partial X}+Pr\left(\frac{\partial^2 U}{\partial X^2}+\frac{\partial^2 U}{\partial Y^2}\right)+RaPr\theta \quad (3)$$

$$\frac{\partial V}{\partial t}+U\frac{\partial V}{\partial X}+V\frac{\partial V}{\partial Y}=-\frac{\partial P_m}{\partial Y}+Pr\left(\frac{\partial^2 V}{\partial X^2}+\frac{\partial^2 V}{\partial Y^2}\right) \quad (4)$$

Conservation of energy:

$$\frac{\partial \theta}{\partial t}+U\frac{\partial \theta}{\partial X}+V\frac{\partial \theta}{\partial Y}=\left(\frac{\partial^2 \theta}{\partial X^2}+\frac{\partial^2 \theta}{\partial Y^2}\right) \quad (5)$$

The mass flow rate is calculated at the entrance of the channel as:

$$Q=\int_0^1 U dY \quad (6)$$

With

$$Ra=\frac{g\beta\Delta T d^3}{a\nu}: \text{Rayleigh number}$$

$$Ra^*=\frac{Ra}{A}: \text{channel Rayleigh number}$$

$$Pr=\frac{\nu}{a}: \text{Pradtl number}$$

Where, the dimensionless variables are:

$$\tau=\frac{\alpha}{d^2}t,\ X=\frac{x}{d},\ Y=\frac{y}{d},\ U=\frac{ud}{a},$$

$$V=\frac{vd}{a},\ \theta=\frac{T-T_0}{T_w-T_0},\ P_m=\frac{(p+\rho gx)d^2}{\rho a^2}$$

Boundary and initial conditions: Figure 1 shows the geometry under consideration in the present investigation with axis system. The wall at the left side is adiabatic and at the right side is maintained at uniform temperature T_w. The fluid is assumed to enter into the channel at ambient temperature T_0, ambient pressure and the mass flow rate given by Eq. (6). At the upper boundary, the streamwise variations of the velocity and temperature are neglected while the pressure is assumed to be equal to the ambient pressure. If the fluid enters by the top of the channel because of a recirculation, it is supposed to be at the ambient temperature. The gravity acceleration g acts vertically downwards. No slip boundary condition is applied for velocity components at vertical walls.

Boundary conditions can be summarized by the following Eq:

$$0\le Y\le 1 \text{ and } X=0 \quad (7)$$
$$\frac{\partial U}{\partial X}=0,\ V=0,\ \theta=0,\ P_m=0$$

$$0\le Y\le 1 \text{ and } X=A \quad (8)$$
$$\frac{\partial \theta}{\partial X}=\frac{\partial U}{\partial X}=\frac{\partial V}{\partial X}=0,\ P_m=0$$

$$0\le X\le A \text{ and } Y=0 \quad (9)$$
$$\frac{\partial \theta}{\partial Y}=0,\ U=0,\ V=0$$

$$0\le X\le A \text{ and } Y=F(X) \quad (10)$$
$$\theta=1,\ U=0,\ V=0$$

As the initial condition, a motionless state and uniform temperature are taken:

$$\text{At } \tau=0,\ 0\le x\le A \text{ and } 0\le Y\le F(X)$$
$$U=V=P_m=\theta=0 \quad (11)$$

Heat transfer: The local heat transfer evaluated at the wall surface of the channel is calculated in terms of local Nusselt number using the following equation:

$$Nu=\frac{h\,d}{\lambda}=\left(\frac{\lambda\frac{\partial T}{\partial n}}{\lambda\frac{\Delta T}{d}}\right)=\left(\frac{\partial \theta}{\partial N}\right)_{Y=F(X)} \quad (12)$$

Local Nusselt numbers based on the channel width are integrated to calculate the global or average value of Nusselt number according to

$$\overline{Nu}=\frac{1}{A}\int_0^A\left(\frac{\partial \theta}{\partial N}\right)_{Y=F(X)} dX \quad (13)$$

Solution methodology: The numerical technique used in the present study is similar to that of Issa (1985) and Issa *et al.* (1991) based on the finite-volume method as described by Patankar (1980). The solution domain is first subdivided into finite number of control volumes (CV). Body fitted, non-orthogonal grids are used. Grids are oriented in such a way that the number of CV is higher near the wall where higher gradients of variable values are expected (Fig. 1). A collocated variable arrangement is used in the present investigation. All variable are calculated at the center of each CV. PISO (Pressure Implicit with Splitting of Operators) algorithm is used to solve the coupled system of governing equations. First

the momentum equations (Eq. 3 and 4) are discretized and linearized. Convective fluxes are approximated using UDS scheme, which is second order accurate. Central differencing scheme (CDS) approximated diffusive fluxes and linear interpolation is used to compute cell-face diffusion coefficients based on cell-center values. Discretized momentum equations lead to an algebraic equation system for velocity components U and V where pressure, temperature, fluid properties are taken from the previous iteration except the first iteration where initial conditions are applied. These linear equations systems are solved iteratively (inner iteration) to obtain an improved estimate of velocity. The improved velocity field is then used to estimate new mass fluxes, which satisfy the continuity equation. Pressure-correction equation is then solved using the same linear equation solver and to the same tolerance. Energy equation is then solved in he same manner to obtain better estimate of new solution. This competes one outer iteration and is repeated until the residual is less than or equal to 10^{-5}. In this study the incomplete factorisation method (also called the incomplete LU decomposition) is used to solve the linear equation systems. To avoid divergence, under-relaxation parameter 0.7 is used for velocity, 0.3 for pressure and 0.8 for temperature.

Accuracy: For reasonably high values of $Ra^*(\geq 100)$, any region outside the channel can be neglected, upstream thermal diffusion through the inlet section being negligible. Thus, because the fluid is not pre-heated before entering, the computational domain can be restricted to the space between the plates.

In the present investigation a non-orthogonal, non-uniform and non-staggered grid system is used. Five combinations (25×100, 30×100, 40×100, 40×120 and 50×140) of control volumes are used to test the effect of grid size on the accuracy of the predicted results. Figure 2 shows the distribution of average Nusselt numbers of the hot wall as a function of grid sizes for four different channel Rayleigh numbers. It is evident from the figure that for lower channel Rayleigh numbers the Nusselt number is independent of the grid sizes studied here and for the higher channel Rayleigh numbers the three higher grid sizes give the same result. Thus, throughout this study the results are presented for 40×100 CVs'.

Predicted results of average Nusselt numbers for a smooth channel with the same boundary conditions are compared with the correlation of Churchill and Usagi (Taine and Petit, 1989). This correlation, valid for low and high values of the channel Rayleigh number, is as follows:

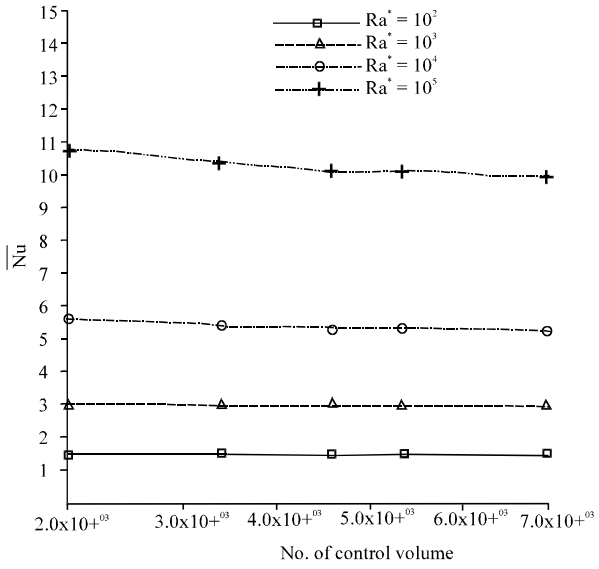

Fig. 2: Average Nusselt number as a function of number of control volume for A = 5, a = 0.450, $L_0 = 1$, $L_1 = 2$

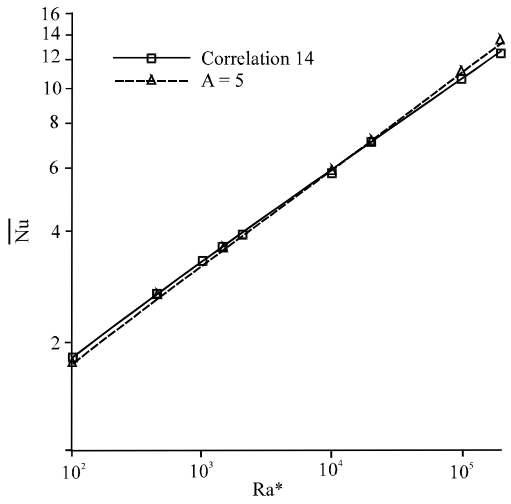

Fig. 3: Variation of the average Nusselt number versus channel Rayleigh number for Pr = 0.71

$$\overline{Nu} = \left[\frac{144}{Ra^{*2}} + \frac{2.873}{Ra^{*0.5}}\right]^{-0.5} \quad (14)$$

Figure 3 shows this comparison. Predicted results show a very good agreement with correlation (14). Thus, this can give us confidence in the numerical simulations reported in what follows.

RESULTS AND DISCUSSION

The focus of this study is to examine the influences upon flow and heat transfer to changes in the geometrical parameters of a single sinusoidal obstruction in an asymmetrically heated vertical channel. Although our theoretical model has an academic character, one can imagine an extension being able to present an interest at the level of practical applications such as the heat exchangers with fins, the applications in electronics such as the girdles of cooling presenting protuberances on their external surfaces , the solar collectors as well as the systems of stocking energy.

The computations were carried out for six values of the sinusoid amplitude describing the obstruction, a = 0.0 to 0.5. Three different aspect ratios were analyzed, A = 3, 5, 10 for a channel Rayleigh number range, $10^2 \leq Ra^* \leq 2.10^5$. This Rayleigh number is defined as the ratio of the Rayleigh number to the aspect ratio of the channel. All the numerical computations were performed for air (Pr = 0.71). The results are presented as isothermal contours and streamlines. The local and average heat transfer coefficients are also calculated.

Flow and thermal field: Figure 4 and 5 show the streamlines and isothermal contours at $Ra^* = 10^3$ and 10^5 for six different amplitudes of the sinusoidal obstruction (a = 0.5 to 0).

As the flow approaches the obstruction, the streamlines are deflected towards the adiabatic wall and therefore, in the partially obstructed region, the streamlines are more densely packed.

Beyond the obstruction, the flow separates and reattaches further downstream on the hot plate.

The isotherm distribution expectedly shows a monotonic decrease of temperature from the hot wall to the adiabatic surface.

Local heat transfer: The local Nusselt number along the hot wall is presented in Fig. 6 for four different channel Rayleigh numbers, $Ra^* = 10^2, 10^3, 10^4$ and 10^5, for a constant amplitude of the sinusoidal obstruction a = 0.375, aspect ratio A = 5 and $L_1 = 2.0$. It is seen from this figure that the local Nusselt number increases with distance up the wall, then decreases and then increases again for all the range of channel Rayleigh numbers investigated. The lowest values of local Nusselt numbers are at the two intersections between the obstruction and the wall. As the velocity of the flow increases in the vicinity of the obstruction, the heat transfer coefficient increases to a maximum value and then decreases further up the channel where the velocity decreases to a minimum value and then increases again. The local Nusselt number is amplified when the channel Rayleigh numbers are increased.

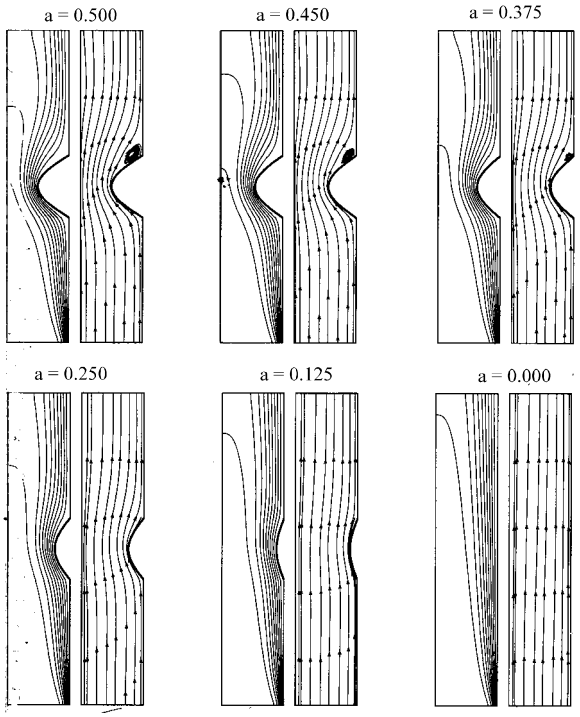

Fig. 4: Isothermal lines (left) and streamlines (right) for A = 5, $L_0 = 1$, $L_1 = 2$ and $Ra^* = 10^3$ for (a) a = 0.500, (b) a = 0.450, (c) a = 0.375, (d) a = 0.250, (e) a = 0.125, (f) a = 0.000

Effect of sinusoidal obstruction: The effect of the obstruction on heat transfer is shown in Fig. 7 and 8 by the curve of local Nusselt numbers along the wall. The profiles of the local Nusselt numbers are presented for four values of the amplitude of the sinusoidal obstruction (a = 0.0, a = 0.125, a = 0.25, a = 0.45) for $Ra^* = 10^3$ and $Ra^* = 10^5$. Since the heat flux transferred to the air decreases with the temperature difference between the wall and the air and the flow velocity is maximum in the portion of the channel where the section is restricted, the local Nusselt number presents a peak at a X-coordinate corresponding to the top of the obstruction. This peak decrease with the amplitude of the obstruction. The flow velocity is more marked for high Rayleigh numbers and consequently the local Nusselt number increases with the amplitude of the obstruction. The Nusselt number falls in the recirculation zones with the increase of the Rayleigh number. Figure 9 shows the variation of the average

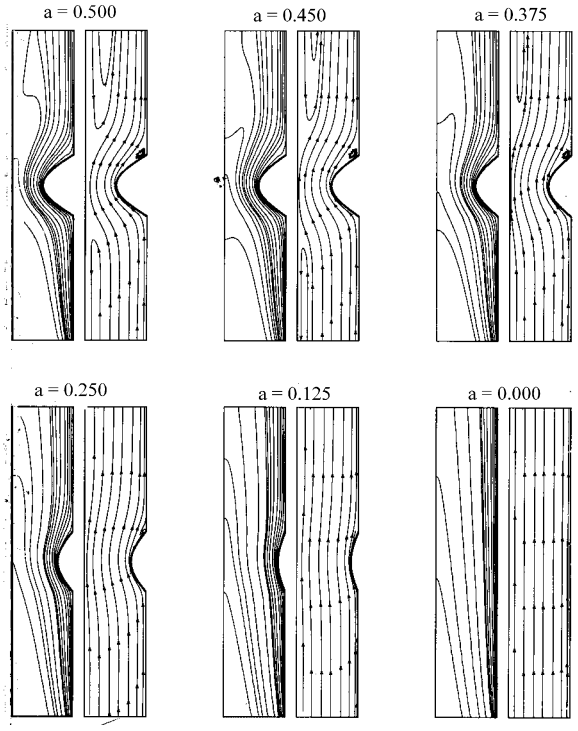

Fig. 5: Isothermal lines (left) and streamlines (right) for A = 5, $L_0 = 1$, $L_1 = 2$ and $Ra^* = 10^5$ for (a) a = 0.500, (b) a = 0.450, (c) a = 0.375, (d) a = 0.250, (e) a = 0.125, (f) a = 0.000

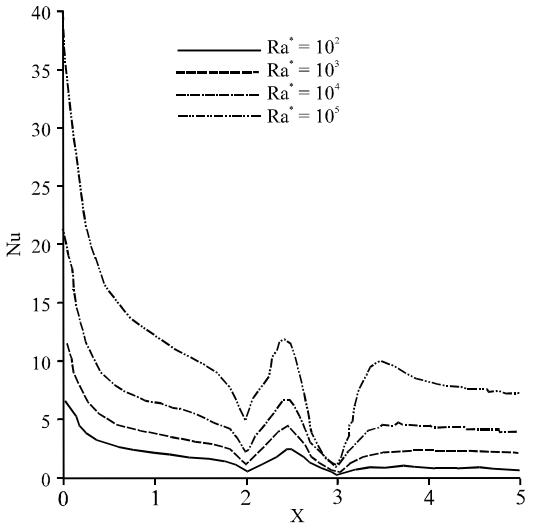

Fig. 6: Local Nusselt number variation with distance along the left wall at different channel Rayleigh number for A = 5, a = 0.375, $L_0 = 1$, $L_1 = 2$

Nusselt numbers as a function of the channel Rayleigh number for various values of the amplitude of the sinusoidal obstruction, while the values of the inlet mass

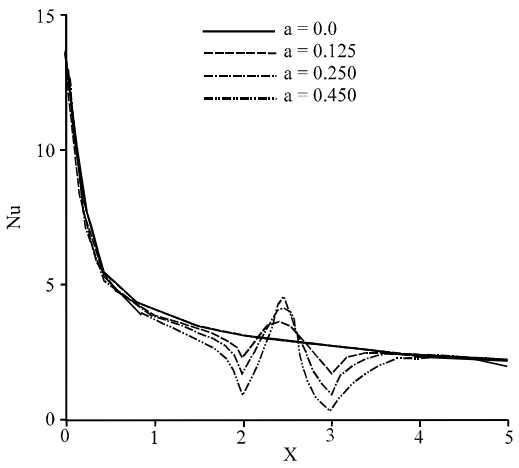

Fig. 7: Local Nusselt number variation with distance along the left wall at different amplitudes of the sinusoidal obstruction for A = 5, $Ra^* = 10^3$, $L_0 = 1$, $L_1 = 2$

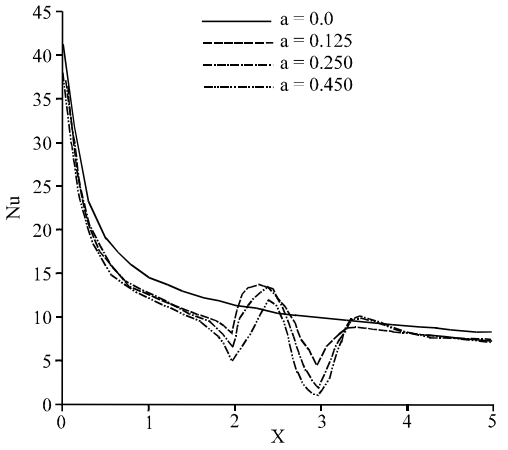

Fig. 8: Local Nusselt number variation with distance along the left wall at different amplitudes of the sinusoidal obstruction for A = 5, $Ra^* = 10^5$, $L_0 = 1$, $L_1 = 2$

flow rate reported in Fig.10. It is obvious that the average Nusselt numbers are largely below those of smooth channel, although the heated surface is greater. The increase of the amplitude (a = 0.0 to 0.5) lead to a loss of average heat transfer about 23%. Clearly, the inlet flow rate of the obstructed channels is significantly lower than that of the unobstructed channel. Increasing the channel Rayleigh number intensifies these trends.

Figure 11 and 12 present the changes in the average Nusselt number and in the mass flow rate as the amplitude of the sinusoidal obstruction increases from 0 to 0.5 for a

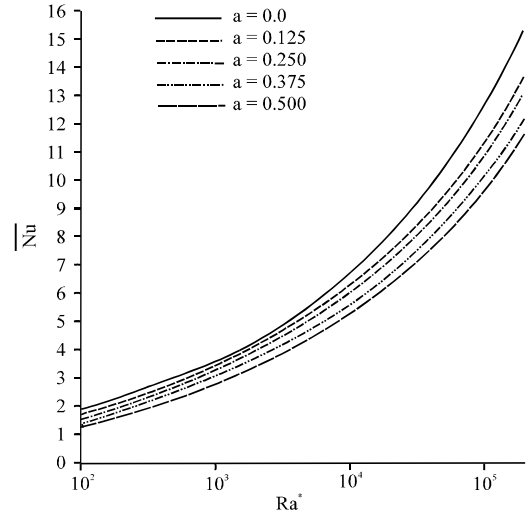

Fig. 9: Variation of the average Nusselt number versus channel Rayleigh number for obstructed channels ($L_0 = 1$, $L_1 = 2$, A = 5)

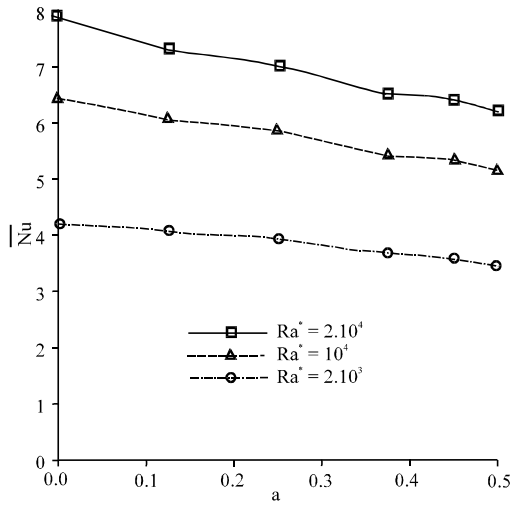

Fig. 11: Variation of the average Nusselt number as a function of the amplitude of the sinusoidal obstruction for three different channel Rayleigh numbers (A = 5, $L_0 = 1$, $L_1 = 2$)

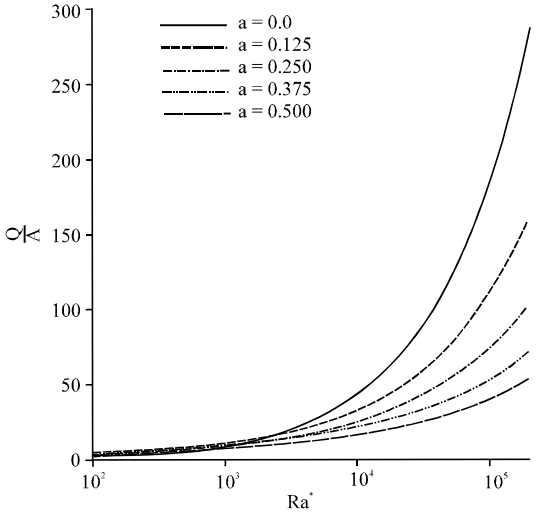

Fig. 10: Variation of the inlet mass flow rate versus channel Rayleigh number for obstructed channels ($L_0 = 1$, $L_1 = 2$, A = 5)

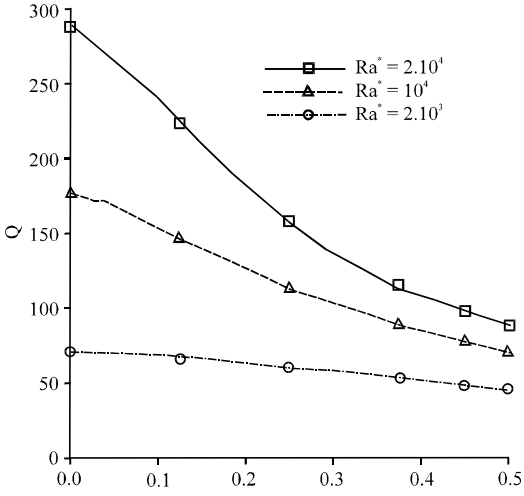

Fig. 12: Variation of the mass flow rate as a function of the amplitude of the sinusoidal obstruction for three different channel Rayleigh numbers (A = 5, $L_0 = 1$, $L_1 = 2$)

fixed obstruction length of 1. The value of Q for all cases decrease while showing the same trend, a sharp decrease for lowest amplitude for the obstruction and a linear decrease from a = 0.25 to 0.5. This decrease is mush greater for greatest value of the channel Rayleigh number.

Obstruction allows having a better local heat transfer (at the level of the obstruction). This transfer decreases when obstruction is moved towards the exit of the canal (Fig.13). For the large values of Rayleigh number the transfer increases but in an almost identical way for the three locations of the obstruction (Fig. 14). This is due to the recirculation zone which appears after the obstruction for these Rayleigh numbers.

Effect of aspect ratio: To study the effect of aspect ratio on the heat transfer rate, the average Nusselt number of the three different geometries is plotted in Fig. 15.The Nusselt number is an increasing function of the Rayleigh number and the aspect ratio A. The exchange surface

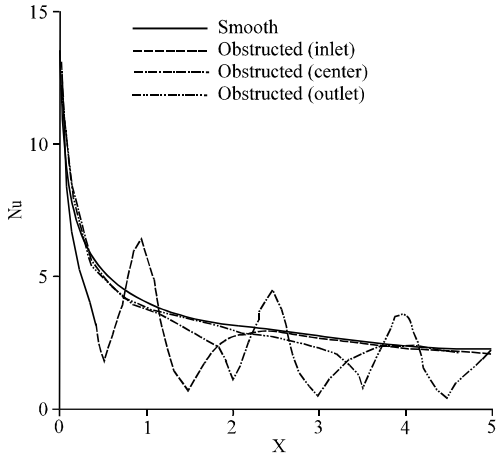

Fig. 13: Local Nusselt number profile along the left wall for three different locations of the sinusoidal obstruction with Ra* = 10^3, A = 5, a = 0.375, L_0 = 1

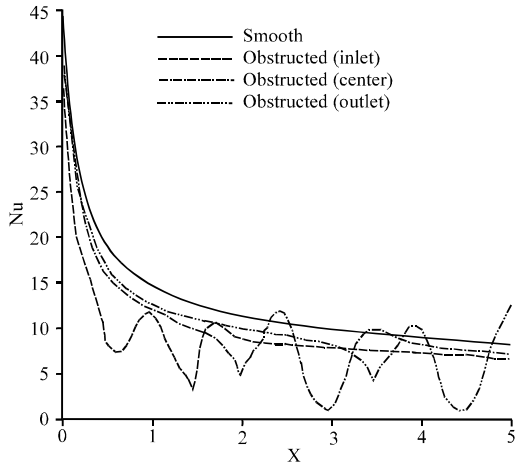

Fig. 14: Local Nusselt number profile along the left wall for three different locations of the sinusoidal obstruction with Ra* = 10^5, A = 5, a = 0.375, L_0 = 1

between the hot wall and the ambient environment is especially important than the aspect ratio is high. The heat transfer between the fluid and the wall being related to this exchange surface, it results from it that the Nusselt number is all the more high as the aspect ratio is important. The average heat transfer at A = 3 is over 34% lower than that for A = 5, while for A = 5 is about 41 % less compared with that for A = 10.

Besides, the vertical velocity believes with A (Fig. 16) Therefore, the thermal exchange, which is proportional at this velocity, is all the more high as the aspect ratio is large.

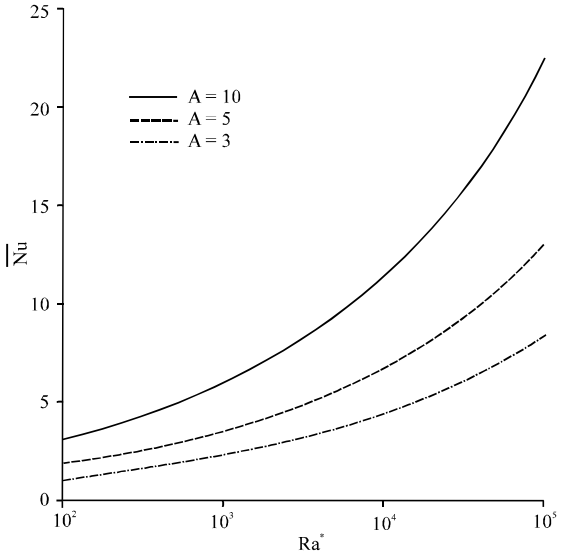

Fig. 15: Variation of average Nusselt number with aspect ratio of the channel for a = 0.250, L_0 = 1, L_1 = 2

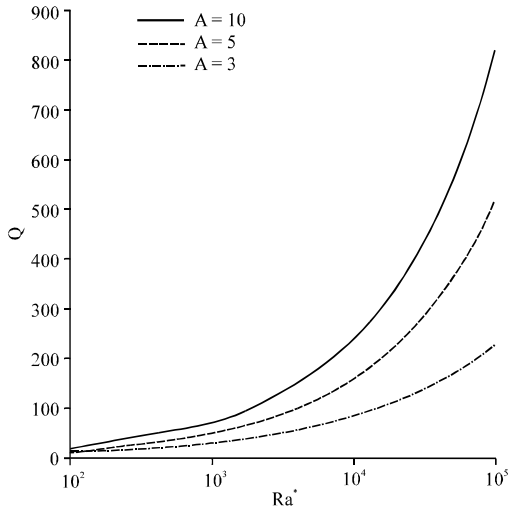

Fig. 16: Variation of the inlet mass flow rate with aspect ratio of the channel for a = 0.250, L_0 = 1, L_1 = 2

Correlation: Although the interest of the present study is to put in evidence the different behavior of the flow and the heat transfer according to various geometrical parameters of the obstructed channel, the results obtained by our numerical simulation can be exploited and presented in a form of correlations which can interest practical environment.

For illustrated well this and by means of the least-square regression analysis, the average Nusselt number $(\overline{Nu})$, for aspect ratio of the channel A = 5 with center

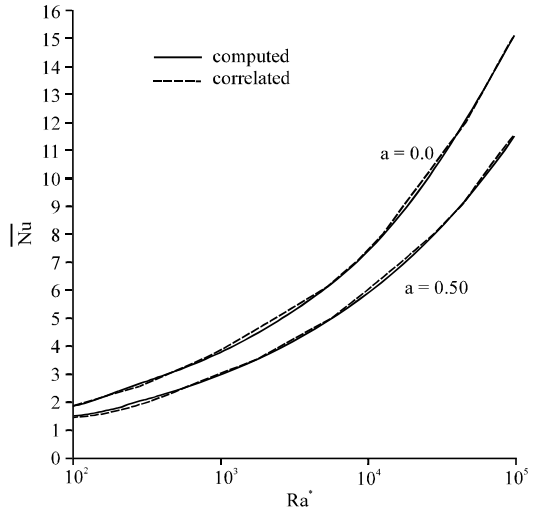

Fig. 17: Comparison of computed and correlated results for average Nusselt number versus channel Rayleigh number for obstructed channels. ($L_0 = 1$, $L_1 = 2$, $A = 5$)

Table 1: Coefficients of Eq. (15)

a_1	b_1	c_1	Standard Error	Correlation coefficient
0.5438	0.2734	0.5897	0.1983	0.9974

location of the obstruction can be correlated well with the channel Rayleigh number (Ra^*) and amplitude of the sinusoidal obstruction (a) of the following form:

$$\overline{Nu} = a_1.Ra^{*.b_1}.c_1^{a} \quad (15)$$

Where the coefficients a_1, b_1 and c_1 are listed in Table 1 for $Ra^* = 10^2 - 2.10^5$ and $A = 5$.

It was found that the correlation must be bifurcated about the amplitude of the sinusoidal obstruction to provide a good fit with the numerical results. Figure 17 shows the typical behavior of $\overline{Nu}$.

The evolution of local Nusselt number was not able to be fitted by using the least squares technique because of its irregular variation due to the presence of the obstruction. To surmount this difficulty, it would have been desirable that the surface of the canal is constituted by sinusoidal obstructions so that the local Nusselt number varies in a regular way. This configuration which can be treated by our simulation code is not the object of this study.

CONCLUSIONS

We deferred some results concerning a numerical study of the influence of a sinusoidal obstruction on the transfers in a channel delimited by two vertical plates for a wide range of Ra. The presence of obstruction in the channel causes better local heat transfer rates due to increments in both the vertical flow and surface area on the obstructed wall. The numerical results show in particular that the influence of the obstruction on the transfers is all the more significant as its amplitude is high. For high values of the Rayleigh number, it appears a recirculation zone located in the higher part of the channel downstream from the obstruction. The local Nusselt number is maximum at the top of the obstruction, zone where the convectifs transfers are most intense. However, the average Nu decreases when compared to that for the unobstructed channel owing to the reduction of mass flow rate and the existence of stagnant region caused by the obstruction.

The performance of the methodology applied in the simulations has been also illustrated in terms of grid independency, computational effort and convergence rates. Nevertheless, the transient behavior at Rayleigh numbers higher than those considered in this work as well as the study of the influence of the aspect ratio of the channel lower than those studied here on the thermal and flow patterns need to be explored in further research. The logical future studies of this topic would consist in:

- To consider a three-dimensional case.
- To study the mixed convection case.
- To study also, the case where the wall of the canal is completely covered with sinusoidal obstructions.

Nomenclature

a	amplitude of the sinusoidal obstruction. a_0 /d
A	aspect ratio of the channel. A = H/d
d	channel width, m
F(X)	geometric function
g	gravitational acceleration, ms^{-2}
h	heat transfer coefficient, $Wm^{-2}K^{-1}$
H	channel height, m
L_0	obstruction length. l_0/d
L1	obstruction location from channel inlet. l_1/d
Nu	local Nusselt number
$\overline{Nu}$	average Nusselt number
P_m	dimensionless motion pressure
Pr	Prandtl number
Q	dimensionless mass flow rate
Ra	Rayleigh number
Ra^*	channel Rayleigh number ($Ra^* = Ra/A$)
T_0	ambient temperature, K
U, V	dimensionless velocity components

X,Y Dimensionless coordinates

Greek symbols

α thermal diffusivity, $m^2.s^{-1}$
β thermal expansion coefficient of fluid, k^{-1}
θ dimensionless temperature
ρ density of fluid
λ thermal conductivity of fluid, $W.m^{-1}.K^{-1}$
ν kinematic viscosity of fluid, $m^2.s^{-1}$
$\triangle T$ temperature difference , K

Subscript

0 at ambient air
w at wall

REFERENCES

Agonaffer, D. and C.B. Watkins, 1985. Numerical solution of natural convection between diverging plates. ASME ., pp: 32.

Aihara, T., 1973. Effects of inlet boundary conditions on numerical solutions of free convection between vertical parallel plates. Report of the Institut High Speed. Mechanics, 28: 1-27.

Akbari, H.T. and R. Borges, 1979. Finite convective laminar flow within Trombe wall channel. Solar Energy, 22: 165-174.

Aung, W., 1972. Fully developed laminar free convection between vertical parallel plates heated asymmetrically. Intl. J. Heat Mass Transfer, 15: 1577-1580.

Aung, W., L.S. Fletcher and V. Sernas, 1972. Development of laminar free convection between vertical plat plates with asymmetric heating. Intl. J. Heat Mass Transfer, 15: 2293-2328.

Aung, W. and G. Worku, 1986a. Developing flow and flow reversal in a vertical channel with asymmetric wall temperatures. ASME. J. Heat Transfer, 108: 299-304.

Aung, W. and G. Worku, 1986b. Theory of fully developed, combined convection including flow reversal. ASME. J. Heat Transfer, 108: 485-488.

Azevedo, L.F.A. and E.M. Sparrow, 1986. Natural convection in a vertical channel vented to the ambient through an aperture in the channel wall. Intl. J. Heat Mass Transfer, 29: 819-830.

Bar-Cohen, A. and W.M. Rohsenow, 1984. Thermally optimum spacing of vertical natural convection cooled, parallel plates. ASME. J. Heat Transfer, 116: 116-123.

Bodoia, J.R. and J.F. Osterle, 1962. The development of free convection between heated vertical plates. ASME. J. Heat Transfer, 84: 40-44.

Dalbert, A.M., J.L. Peupe, F. Penot and J.F. Robert, 1980. Etude de l'Ecoulement dans un collecteur plan. Revue Phys. Applied, 15: 201-206.

Dalbert, A.M., F. Penot and J.L. Peube, 1981. Convection naturelle laminaire dans un canal vertical chauffé à flux constant. Intl. J. Heat and Mass Transfer, 24: 1463-1473.

Desrayaud, G. and A. Fichera, 2002. Laminar natural convection in a vertical isothermal channel with symmetric surface-mounted rectangular ribs. Intl. J. Heat and Fluid Flow, 23: 519-529.

Dyer, J.R. and J.H. Fowler, 1966. The development of natural convection in a partially-heated vertical channel formed by two parallel surfaces. Mech. Chem. Eng. Trans. Inst. Engrs., Aust. MC2, pp: 78-86.

Dyer, J.R., 1975. The development of laminar natural convective flow in a vertical uniform heat flux duct. Intl. J. Heat and Mass Transfer, 18: 1455-1465.

Dyer, J.R., 1978. Natural convective flow through a vertical duct with a restricted entry. Intl. J. Heat and Mass Transfer, 21: 1341-1354.

Elenbaas, W., 1942. Heat dissipation of parallel plates by free convection. Physica, 9: 1-28

Engel, R.K. and W.K. Mueller, 1967. An analytical investigation of natural convection in vertical channels. ASME., pp: 16.

Habchi, S. and S. S. Acharrya, 1986. Laminar mixed convection in a partially blocked, vertical channel. Intl. J. Heat and Mass Transfer, 29: 1711-1722.

Hadjadj, A. and M. Kyal, 1999. Effect of two sinusoidal protuberances on natural convection in a vertical concentric annulus. Numerical Heat Transfer, 36: 273-289.

Hugot, G., 1972. Etude de la convection naturelle entre deux plaques planes, verticales, parallèles et isothermes. Entropie, pp: 55-66.

Issa, R.I., 1985. Solution of the implicitly discretized fluid flow equations by operator-splitting. J. Comp. Phys., 62: 40-65.

Issa, R.I., B. Ahmadi-Befrui, K.R. Beshay and A.D. Gosman, 1991. Solution of the implicitly discretized reacting flow equations by operator-splitting. J. Comp. Phys., 93: 388-410.

Kettleborough, C.F., 1972. Transient laminar free convection between heated vertical plates including entrance effects. Intl. J. Heat and Mass Transfer, 15: 883-896.

Marcondes, F. and C.R. Maliska, 1999. Treatment of the inlet boundary conditions in natural convection flows in open-ended channels. Num. Heat Transfer, 35: 317-345.

Mehrotra, A. and S. Acharya, 1993. Natural convection heat transfer in smooth and ribbed vertical channels. Intl. J. Heat and Mass Transfer, 36: 236-241.

Miyatake, O. and M. Fujii, 1972. Free convective heat transfer between vertical parallel plates, one plate isothermally heated and the other thermally insulated. Heat Transfer-Jap. Res., 3: 30-38.

Nakamura, H., Y. Asako and T. Naitou, 1982. Heat transfer by free convection between two parallel plat plates. Num. Heat Transfer, 5: 95-106.

Naylor, D., J.M. Floryan and J.D. Tarasuk, 1991. A numerical study of developing free convection between isothermal vertical plates. ASME. J. Heat Transfer, 113: 620-626.

Ostrach, S., 1952. Laminar natural convection flow and heat transfer of fluids with and without heat sources in channels with constant wall temperatures. NACA. Tech. Note, pp: 2863.

Patankar, S.V., 1980. Numerical Heat Transfer and Fluid Flow. Mac Graw-Hill, New York.

Penot, F. and A.M. Dalbert, 1983. Convection naturelle mixte et forcée dans un thermosiphon vertical chauffé à flux constant. Intl. J. Heat and Mass Transfer, 26: 1639-1647.

Said, S.A.M. and R.J. Krane, 1990. An analytical and experimental investigation of natural convection heat transfer in vertical channels with a single obstruction. Intl. J. Heat and Mass Transfer, 33: 1121-1134.

Sparrow, E.M. and W.Q. Tao, 1982. Buoyancy driven fluid flow and heat transfer in a pair of interacting vertical parallel channels. Num. Heat Transfer, 5: 39-58.

Sparrow, E.M., G.M. Chrysler and L.F.A. Azevedo, 1984. Observed flow reversals and measured-predicted Nusselt numbers for natural convection in a one-sided heated vertical channel. ASME. J. Heat Transfer, 106: 325-332.

Sparrow, E.M. and L.F.A. Azevedo, 1985. Vertical-channel natural convection spanning between the fully-developed limit and the single plate boundary layer limit. Intl. J. Heat and Mass Transfer, 28: 1847-1857.

Sparrow, E.M., R. Ruiz and L.F.A. Azevedo, 1988. Experiments and numerical investigation of natural convection in convergent vertical channels. Intl. J. Heat and Mass Transfer, 31: 907-915.

Sparrow, E.M. and R. Ruiz, 1988. Experiments on natural convection in divergent vertical channels and correlation of divergent, convergent and parallel-channel Nusselt numbers. Intl. J. Heat and Mass Transfer, 31: 2197-2205.

Taine, J. and J.P. Petit, 1998. Transferts Thermiques, Mécanique Des Fluides Anisothermes. 2nd Edn., Dunod, Paris, pp: 363-364.

Viswatmula, P. and M. Ruhul Amin, 1995. Effects of multiple obstructions on natural convection heat transfer in vertical channels. Intl. J. Heat and Mass Transfer, 38: 2039-2046.

Webb, B.W. and D.P. Hill, 1989. High Rayleigh number laminar natural convection in an asymmetrically heated vertical channel. ASME. J. Heat Transfer, 111: 649-656.

Wirtz, R.A. and R.J. Stutzman, 1982. Experiments on free convection between vertical plates with symmetric heating. ASME. J. Heat Transfer, 104: 501-507.